Addition of Lysines to the 50/20 kDa Junction of Myosin Strengthens Weak Binding to Actin without Affecting the Maximum ATPase Activity†

Peteranne B. Joel,‡ H. Lee Sweeney,§ and Kathleen M. Trybus*,‡

Department of Molecular Physiology and Biophysics, University of Vermont College of Medicine, Burlington, Vermont 05405-0068, and Department of Physiology, University of Pennsylvania School of Medicine, Philadelphia, Pennsylvania 19104-6085

Received March 17, 2003; Revised Manuscript Received June 4, 2003

ABSTRACT: Much interest has centered on two surface loops in the motor domain to explain the differences in enzymatic and mechanical properties of myosin isoforms. We showed that two invariant lysines at the C-terminal end of loop 2, which is part of the actin-binding interface, are required to obtain actin activation [Joel et al. (2001) *J. Biol. Chem. 276*, 2998−3003]. Here we investigate the effects of increasing positive charge in the variable portion of loop 2 of smooth muscle heavy meromyosin (smHMM). Increasing the net positive charge by +4 increased the affinity for actin in the presence and absence of ATP. The K_m for actin-activated ATPase activity decreased 15-fold, but V_{max} was unchanged, showing that "weak binding" of myosin for actin can be significantly strengthened without increasing the rate-limiting step for V_{max}. The mutant HMM had slower rates of in vitro motility and ADP release compared to WT HMM. ADP release and motility, which were both salt-dependent, correlated linearly with each other. Loop 2 thus plays a major role in setting the affinity for actin but also affects ADP release and motility. Because the actin- and nucleotide-binding regions communicate, mutations to one region can impact multiple facets of myosin's mechanical and enzymatic properties.

Muscle contraction is the result of a cyclic interaction of myosin with actin coupled to ATP hydrolysis. After hydrolysis of ATP by myosin in the dissociated state, actin and myosin form a weakly bound state governed by electrostatic interactions. Progression to a strongly bound actomyosin state is closely associated with P_i release, major conformational changes in myosin, and force generation. ADP release follows. Rebinding of ATP causes dissociation of actin from myosin and initation of a new cycle (reviewed in refs *1* and *2*). The release of P_i is thought to be the rate-limiting step in the ATPase cycle, while the rate of ADP release is thought to determine the rate at which myosin can move actin (*3*, *4*).

Myosin has two flexible surface loops which are the sites of tryptic cleavage of the motor domain into segments of 25, 50, and 20 kDa. Loop 1 (25/50 kDa junction) is near the nucleotide-binding pocket, and loop 2 (50/20 kDa junction) lies at the actin-binding interface. Numerous studies indicate that the initial weak binding of myosin to actin is an electrostatic interaction between positively charged lysine residues in loop 2 and negatively charged residues in subdomain 1 of actin (e.g., refs *5*−*11*). Removal of negative charge from subdomain 1 of actin decreases the affinity of actin for myosin in the presence of MgATP, while relocation of the charge in this subdomain does not alter actomyosin function, consistent with limited stereospecificity of the weak binding interaction (*12*−*14*).

Residues in loop 2 and adjacent to it (L634, F656, R657, T658, Q661) also have a high probability of interaction with actin in the strong binding actomyosin states, based on docking of crystal structures into 3D reconstructions of actin decorated with the smooth muscle myosin head (*15*). Thus loop 2 appears to be a critical part of the actomyosin interface throughout the ATPase cycle. Consistent with this idea, deletion of two invariant lysines (K652/653) at the C-terminal portion of loop 2 abolished both actin-activated ATPase activity and motility. The major functional defect of this mutant was its inability to progress from the weak to the strong binding state, while other steps in the cycle remained unaffected (*16*). We concluded that the conserved lysines are essential trigger residues for actin activation.

Myosin's two loops have been proposed to have distinct functions: loop 1 has been proposed to control the rate of ADP release while loop 2 has been proposed to set the maximum actin-activated ATPase rate (V_{max}) (*17*, *18*). This hypothesis was supported by data which suggested that the actin-activated ATPase activity of loop 2 chimeras correlated with the actin-activated ATPase activity of the loop 2 donor (*19*−*21*). Subsequent studies that methodically investigated the effect of charge changes in loop 2 concluded that positive charge significantly strengthened the affinity of myosin for actin and, to a lesser extent, increased V_{max} (*10*). Severe truncation of the length of loop 2, which is already relatively small in *Dictyostelium* myosin, decreased actin affinity and actin-activated ATPase activity (*11*). Similar studies on loop

† This work was supported by National Institutes of Health Grants AR47906 to K.M.T. and AR35661 to H.L.S.

* To whom correspondence should be addressed at the University of Vermont College of Medicine, Health Science Research Facility 130, Burlington, VT 05405. Telephone: 802-656-8750. Fax: 802-656-0747. E-mail: trybus@physiology.med.uvm.edu.

‡ University of Vermont.

§ University of Pennsylvania.

10.1021/bi034415j CCC: $25.00
Published on Web 07/09/2003

2 were performed with smooth muscle HMM[1] to test the generality of these conclusions. Chimeras of smHMM containing loop 2 from cardiac or skeletal muscle myosin (or variations of these loops) showed an increased affinity for actin compared to WT, but V_{max} was either unaltered or only slightly increased (*22*, *23*).

It has been difficult to definitively conclude whether loop 2 modulates both K_m and V_{max} or only K_m. High K_m values always preclude an accurate determination of V_{max}. Constructs with increased V_{max} values consistently had lower K_m values, leading one to question if affinity and maximal activity are coupled or if conclusions about V_{max} were based on inaccurate extrapolations because of high K_m values.

Here we increased the positive charge in the variable portion of loop 2 of smHMM by addition of three lysines and removal of a glutamic acid, without changing its length. The mutant bound more tightly to actin, but the maximal actin-activated ATPase was the same as WT HMM. Surprisingly, the mutation also slowed ADP release and in vitro motility. We conclude that while the major role of loop 2 is to set the affinity for actin, it can also affect the rate of transitions at the more distant active site.

MATERIALS AND METHODS

Plasmid Construction. The cDNA for chicken gizzard smooth muscle myosin was truncated after the nucleotides coding for amino acid 1112 to create an HMM-like fragment. Nucleotides coding for a myc epitope (*24*) followed by the FLAG epitope (DYKDDDDK) and a stop signal were appended. The HMM-like construct was subcloned into the baculovirus transfer vector pVL1393 (Gibco Invitrogen Corp., Grand Island, NY). Site-directed mutagenesis was used to create a mutant construct (+3K) in which residues 640−645 in loop 2 were mutated from **MTESSL** in the wild-type (WT) HMM to **KTGKKG** in the mutant, thereby introducing three additional lysines and removing one negatively charged residue (E) without a change in length.

Expression and Purification of Proteins. Recombinant baculovirus encoding the HMM-like constructs was prepared by conventional protocols (*25*). Sf9 insect cells in suspension culture were coinfected with virus coding for either the WT HMM or the +3K mutant HMM construct and for virus coding for both smooth muscle regulatory (RLC) and essential (ELC) light chains [in p2Bac vector (Gibco Invitrogen)]. Three days after infection, Sf9 cells were lysed in 10 mM sodium phosphate, pH 7.2, 0.6 M NaCl, 5 mM $MgCl_2$, 3 mM NaN_3, 7% sucrose, 2 mM EGTA, 1% Nonidet P-40, 2 mM MgATP, 4 mM DTT, and protease inhibitors. Protein that fractionated between 40% and 70% ammonium sulfate was dialyzed in the presence of RNase A (Sigma-Aldrich Co., St. Louis, MO; pretreated with protease inhibitors). The HMM was isolated on an anti-FLAG affinity column (Sigma-Aldrich), eluted with FLAG peptide (Sigma-Aldrich), and dialyzed against 10 mM imidazole, pH 7.0, 100 mM NaCl, 1 mM NaN_3, 1 mM $MgCl_2$, 1 mM DTT, 1 μg/mL leupeptin, and 50% glycerol. The RLC on HMM was phosphorylated by addition of ATP, Ca^{2+}, calmodulin, and myosin light chain kinase at 0 °C. The phosphorylated HMM was again dialyzed against the same buffer. The purity of the preparation was determined with SDS−PAGE (*26*). Phosphorylation of the RLC was confirmed using a 40% glycerol gel with the HMM dissolved in 7.5 M urea (*27*). HMM concentration was determined with Bradford reagent (Bio-Rad Laboratories, Hercules, CA) with BSA as a standard.

In Vitro Motility Assay. Phosphorylated HMM at 0.1 mg/mL was mixed with 0.04 mg/mL actin and 1 mM MgATP and centrifuged for 20 min at 350000*g* to remove HMM which was unable to dissociate from actin in the presence of ATP. The motility assay was performed at 30 °C in 25 mM imidazole, pH 7.5, 25 mM KCl, 4 mM $MgCl_2$, 1 mM EGTA, 0.5% methylcellulose, 1 mM MgATP, 1 mM DTT, 3 mg/mL glucose, 0.1 mg/mL glucose oxidase (Sigma-Aldrich), and 0.018 mg/mL catalase (Sigma-Aldrich) (*28*). Assays were also conducted with 60−180 mM KCl and 0.7% methylcellulose. An anti-rod monoclonal antibody (Ab S2.1) (*29*) was used to bind the HMM to the nitrocellulose-coated coverslip.

ATPase Assays. Actin-activated ATPase activity was measured at 37 °C in 8 mM KCl, 10 mM imidazole, pH 7.0, 1 mM DTT, 1 mM NaN_3, 1 mM $MgCl_2$, 1 mM EGTA, and 10 μg/mL HMM. In samples without actin, the HMM concentration was 50 μg/mL. The actin, which was added at 1−60 μM, was pretreated with gelsolin at a molar ratio of 1:17 (gelsolin:actin). Gelsolin was used to decrease the viscosity of actin so that mixing would be more efficient at high actin concentrations, thus ensuring a linear time course for phosphate release. The reactions were initated by the addition of 2 mM MgATP. The reactions were stopped with SDS at six time points per actin concentration, and inorganic phosphate was determined colorimetrically (*30*). NH_4^+-ATPase activity was measured at 37 °C in 0.4 M NH_4Cl, 2 mM EDTA, 25 mM Tris−base, pH 7.5, 0.2 M sucrose, and 1.5 μg/mL HMM. The reactions were initated by addition of 4 mM NH_4ATP. The reactions were stopped at six time points with SDS, and inorganic phosphate was determined colorimetrically.

Cosedimentation Assay for Weak Binding. Varying concentrations of actin [pretreated with a 1.5 molar excess of phalloidin (Sigma-Aldrich)] were mixed with 0.15 mg/mL HMM, 0.15 mg/mL BSA, and 3 mM MgATP in 5 mM imidazole, pH 7.0, 20 mM KCl, 2 mM DTT, and 1 mM $MgCl_2$ at 4 °C. The samples were centrifuged in the Beckman TL-100 at 350000*g* for 15 min at 4 °C. Equal proportions of supernatant and dissolved pellet were run on 12% SDS−PAGE. The gels were stained with Coomassie Brilliant Blue R. Gel images were captured in digital format using a Kodak Digital Science DC120 zoom digital camera. The band intensities were quantified using the Kodak Digital Science 1D image analysis software package to determine the percent of HMM bound to pelleted actin. A plot of band intensity versus micrograms of HMM per lane gave a linear relationship over the range of band intensities found in the experimental samples.

Transient Kinetics. Nucleotide stocks were prepared with an equimolar concentration of magnesium. The ADP release rate (25−180 mM KCl) was measured by mixing an actoHMM·ADP complex (1 μM actoHMM, 100 μM MgADP) with 2 mM MgATP in a Kin-Tek stopped-flow spectropho-

[1] Abbreviations: smHMM, smooth muscle heavy meromyosin; WT, wild type; RLC, regulatory light chain; S1, myosin subfragment 1; DTT, dithiothreitol; SDS−PAGE, sodium dodecyl sulfate−polyacrylamide gel electrophoresis; HCM, hypertrophic cardiomyopathy.

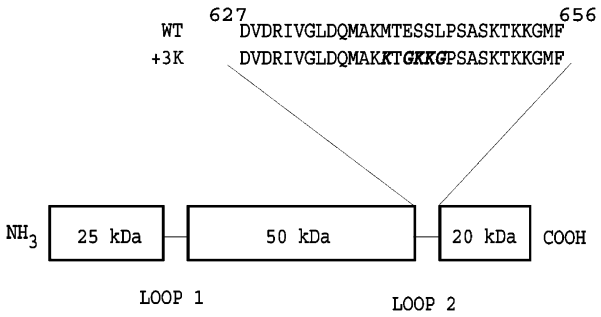

FIGURE 1: Schematic illustrating the location and sequence of loop 2 in wild-type smHMM (WT) and +3K mutant smHMM (+3K). 25, 50, and 20 kDa define the tryptically derived fragments. The loop 2 amino acids shown for WT HMM are amino acids 627−656. The +3K mutant HMM has the amino acids at positions 640, 643, and 644 mutated to lysines, and the amino acids at positions 642 and 645 mutated to glycines (indicated in boldface italics).

tometer. Binding of actin to HMM (90 mM KCl) was measured by mixing 0.5 μM HMM with various excess concentrations of actin. Both rates were determined at 30 °C (25 mM imidazole, pH 7.5, 4 mM $MgCl_2$, 1 mM EGTA, 1 mM NaN_3, 1 mM DTT, and KCl as indicated). These conditions are equivalent to that used for motility. ADP release was also measured at 20 °C (10 mM HEPES, pH 7.0, 5 mM $MgCl_2$, 1 mM EGTA, 1 mM NaN_3, 1 mM DTT, and 25−180 mM KCl). To detect the light scattering signal, the exciting beam (100 W mercury lamp) was passed through a 294 nm interference filter, and the emission was detected with a 294 nm interference filter. Two to four transients were averaged before being fitted to a rate constant, using KinTek software. Single-exponential data were fit to the equation $y = c + a[\exp(-\lambda t)]$ where c is a constant, a is the amplitude of the signal, and λ is the rate constant.

Steady-State Kinetics. The rate of HMM release from actin was determined by mixing pyrene actin−HMM (0.8 μM) with a 20-fold molar excess of unlabeled actin. Actin was labeled with pyrene as described (*28*). The increase in fluorescence was measured as a function of time at 30 °C (25 mM imidazole, pH 7.5, 4 mM $MgCl_2$, 1 mM EGTA, 1 mM NaN_3, 1 mM DTT, 90 mM KCl) and fit to a single exponential. Fluorescence measurements were performed on an ISS Inc. spectrofluorometer (Model ISS K2; ISS Inc., Champaign, IL) equipped with a 300 W xenon arc lamp as an excitation source. Pyrene fluorescence was excited at 365 nm (4 nm bandwidth), and emission was collected with a 400 nm cutoff filter. Data were recorded in ratio mode at 60−120 s intervals (5 s integration time).

RESULTS

Description of the Constructs. WT HMM and +3K mutant HMM constructs derived from chicken gizzard smooth muscle myosin were coexpressed with light chains in a baculovirus/Sf9 cell system. Loop 2 of the +3K mutant HMM was engineered to contain three additional lysines (K) and one less negative charge (E) compared to WT loop 2, creating a net charge change of +4 in the mutant loop 2 (Figure 1). The yield of WT HMM was about 2 mg/billion cells; +3K mutant HMM yielded about 0.5 mg/billion cells. The HMM constructs showed no major contaminants on SDS−PAGE and were indistinguishable from each other in their heavy and light chain components. The mutant construct, like WT HMM, was regulated by light chain phosphorylation.

Table 1: NH_4^+-ATPase Activity of WT and Mutant HMMs[a]

HMM construct	rate (s^{-1})
WT	32 ± 5
+3K	33 ± 5

[a] Values are averages ± SD of three assays with three independent preparations of each HMM (at 37 °C).

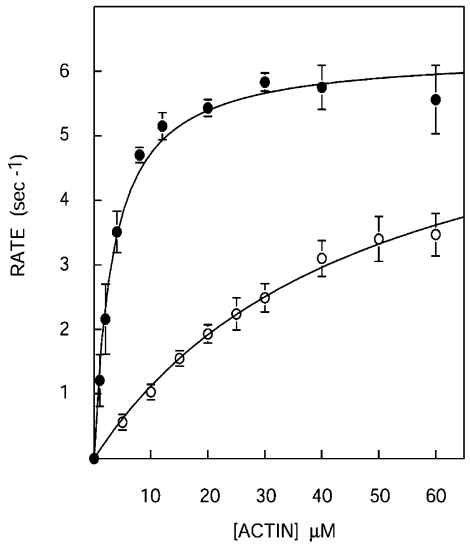

FIGURE 2: Actin-activated ATPase activity of phosphorylated smHMM. Shown are WT HMM (○) and +3K mutant HMM (●). Values are averages of four assays with two independent preparations of each HMM. Data were fit to the Michaelis−Menten kinetic model. V_{max} was 6.5 ± 0.4 s^{-1} for WT HMM and 6.3 ± 0.2 s^{-1} for +3K mutant HMM. K_m was 48 ± 5 μM for WT HMM and 3.3 ± 0.4 μM for +3K mutant HMM.

Addition of Lysines to Loop 2 Decreases K_m without Changing V_{max}. We first established that the WT and +3K mutant HMM constructs had the same NH_4^+-ATPase activity (Table 1), indicating that the mutation does not alter the intrinsic catalytic ATPase function in the absence of actin. The actin-activated ATPase activity of phosphorylated WT and +3K mutant HMMs was then measured as a function of actin concentration (Figure 2). The K_m for the +3K mutant HMM was 15-fold lower than the K_m for WT HMM (3.3 ± 0.4 versus 48 ± 5 μM). Thus the addition of three lysines into loop 2 substantially increased the affinity of the HMM for actin. In contrast, the extrapolated V_{max} values obtained from the illustrated best fit curves were approximately the same for WT and +3K mutant HMM (6.5 ± 0.4 and 6.3 ± 0.2 s^{-1}, respectively). Thus the additional positive charge in loop 2 created a large increase in affinity for actin without appreciably altering the maximum actomyosin ATPase activity.

Addition of Lysines to Loop 2 Strengthens Binding to Actin in the Presence and Absence of Nucleotide. To determine whether the addition of lysines to loop 2 affects the weak binding affinity for actin, cosedimentation assays were performed. Phosphorylated WT and +3K mutant HMMs were cosedimented with increasing concentrations of actin in the presence of 3 mM MgATP (Figure 3). These experiments were conducted at 20 mM KCl to prevent sedimentation of the +3K mutant which occurred at lower

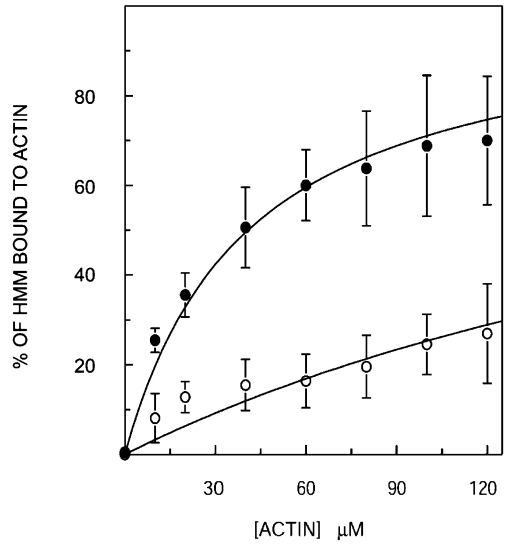

FIGURE 3: Cosedimentation assays of phosphorylated smHMM with actin in the presence of ATP. 0.15 mg/mL WT HMM (○) or +3K mutant HMM (●) was centrifuged in the presence of 3 mM MgATP with 0−120 μM actin. Pellets and supernatant were analyzed by SDS−PAGE. Values are averages ± SD for three assays with two independent preparations of each HMM. The K_d values from these curves, which assume 100% binding at infinite actin concentration, are 255 ± 28 μM for WT HMM and 36 ± 2 μM for +3K mutant HMM.

Table 2: Rates of Actin Binding and Release[a]

HMM construct	k_{on} (M^{-1} s^{-1})	k_{off} (s^{-1})	K_d (nM)
WT	2.5×10^6	1.1×10^{-3}	0.44
+3K	7.3×10^6	0.56×10^{-3}	0.08

[a] Conditions: 25 mM imidazole, pH 7.5, 4 mM $MgCl_2$, 1 mM EGTA, 1 mM NaN_3, 1 mM DTT, 90 mM KCl, 30 °C.

concentrations of KCl in the absence of actin. The K_d values from these curves are 255 ± 28 μM for WT HMM and 36 ± 2 μM for +3K mutant HMM. Thus the additional lysines in loop 2 substantially increase weak binding of HMM to actin.

The rate of binding of mutant and WT HMM to actin in the absence of ATP was measured in the stopped-flow apparatus as a function of actin concentration. The mutant HMM showed an ≈3-fold faster rate of binding to actin (Table 2). The rate of dissociation of HMM from actin was also determined by mixing a pyrene actin−HMM complex with an excess of unlabeled actin and observing the increase in fluorescence as a function of time. The mutant showed an ≈2-fold decrease in the rate at which it dissociates from actin (Table 2). Taken together, the mutant has a 5−6-fold higher affinity for actin than WT HMM in the absence of nucleotide (Table 2).

In Vitro Motility and the ADP Release Rate of +3K Mutant HMM Are Slower than Those of WT HMM. In vitro motility assays of actin filaments sliding over phosphorylated HMM were performed over a range of KCl concentrations to determine whether the lysines added to loop 2 of HMM affect the ability of the HMM to move actin (Figure 4A). Interestingly, the +3K mutant HMM moved actin filaments at a substantially slower rate at 25−100 mM KCl than did the WT HMM. As the KCl concentration was further increased to 120−180 mM, the rate of movement of the actin filaments by +3K mutant HMM became equal to and finally surpassed the rate of movement of actin filaments by WT HMM.

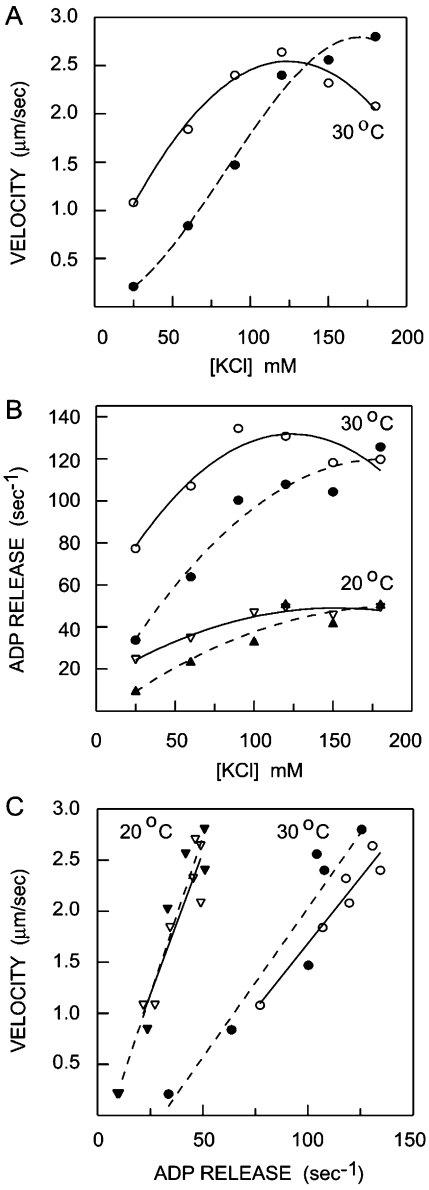

FIGURE 4: (A) Velocity of actin filaments sliding in the in vitro motility assay over phosphorylated smHMM for WT HMM (○) and +3K mutant HMM (●) at 30 °C. The assays performed in 25 mM KCl had 0.5% methylcellulose; assays at higher KCl concentrations had 0.7% methylcellulose. Values are the average of two assays with two independent preparations of each HMM. (B) Rate of ADP release from actoHMM for WT HMM (○, ▽) and +3K mutant HMM (●, ▲) at 20 °C and at 30 °C (see Materials and Methods). Two preparations of each HMM were used in the assays. (C) Correlation of in vitro motility with the rate of ADP release for WT HMM (○, ▽) and +3K mutant HMM (●, ▼). The data for in vitro motility at 30 °C (panel A) were plotted versus the data for ADP release at 20 °C and at 30 °C (panel B).

The rate of ADP release was examined as a possible explanation for the decreased motility of the +3K mutant HMM at low KCl concentration. The rate of ADP release was measured as a function of KCl concentration at 20 °C (the conventional temperature for measuring transient kinetic rates) and at 30 °C (the temperature at which the motility was measured). ActoHMM·ADP was rapidly mixed with MgATP in a stopped-flow apparatus. Dissociation of the

actoHMM complex by MgATP is rate-limited by ADP dissociation, so the rate of the decrease in light scattering measures the rate of ADP release. At 25−100 mM KCl, the rate of ADP release from the +3K mutant HMM was lower than the rate of ADP release from the WT HMM (Figure 4B). At higher KCl concentrations, the rate of ADP release from the +3K mutant and WT HMM became essentially identical. The slower rate of ADP release from the +3K mutant HMM at low ionic strength thus accounts for the lower motility of the +3K mutant HMM. The rate of ADP release showed a linear correlation with the rate of in vitro motility (Figure 4C) for both WT and mutant HMM, consistent with this molecular step being rate-limiting for movement.

DISCUSSION

Role of Loop 2. The primary role of loop 2 is to set the affinity for actin, both in the presence and in the absence of nucleotide. Increasing the positive charge of loop 2 of smHMM by only +4 caused the mutant HMM to have a 15-fold lower K_m in actin-activated ATPase assays, without significantly altering V_{max}. Binding assays confirmed that the mutant HMM's affinity for actin was increased both in the presence (7-fold increase) and in the absence (5−6-fold increase) of nucleotide.

Several studies are consistent with the idea that the net charge of loop 2 controls actin affinity. Deletion of 16 residues from loop 2 of smHMM increased the net charge by +1 and caused a 4-fold decrease in K_m with no change in V_{max} (*16*). Systematic increases in the positive charge of loop 2 of the *Dictyostelium* motor domain caused a marked reduction in the K_m for the actin-activated ATPase (*10*). Conversely, reduction of the positive charge of loop 2 in myosin V by +3 caused a 5-fold increase in K_m, but again V_{max} was unaffected (*31*). Mutation of any of three positive charges in loop 2 of *Dictyostelium* myosin to alanines increased K_m without a significant change in V_{max} (*32*). These results are consistent with the idea that the initial weak binding between myosin and actin involves interaction of the lysines in loop 2 with negatively charged residues in subdomain 1 of actin and suggests that the net charge of loop 2 is a primary determinant of myosin's affinity for actin. These experiments also suggest that altering the strength of the weak binding interaction does not by itself modulate V_{max}.

The experiments performed with *Dictyostelium* myosin agree with our results that loop 2 affects the strength of actomyosin interactions, but some of those experiments also suggest that V_{max} is affected. The mutational studies with *Dictyostelium* have in general involved larger changes in sequence and in length than those performed with smooth muscle HMM. The native loop 2 of *Dictyostelium* myosin is shorter than loop 2 of most other myosins and therefore may show more effects on function when extensive mutations are made. When myosins with similar kinetics are compared, an evolutionary analysis shows that the sequences of the loop regions are in fact more constrained than the sequences of the rest of the molecule (*33*). Alternatively, some of the differing conclusions may be attributed to inaccurate extrapolations of V_{max} values when the K_m for actin is high.

Role of Loop 1. Loop 1 affects ADP release and in vitro motility as originally postulated (*17*), but several studies show that loop 1 can also modulate V_{max}. Smooth muscle has two isoforms of loop 1 that differ by the presence or absence of a seven amino acid insert. The presence of the insert increases the rate of ADP release and in vitro motility but also doubles V_{max} of the actin-activated ATPase activity (*34*−*37*). Similarly, the striated and catch muscle myosins of the scallop *Placopecten* are almost identical except at loop 1, and yet these myosins differ significantly in their actin-activated ATPase activity as well as their rate of in vitro motility (*38*, *39*). The possibility that other residues contribute to the change in ATPase activity remains open for the scallop myosins that are derived from tissue. Results obtained with *Dictyostelium* myosin differed: loop 1 chimeras affected ADP release and in vitro motility but had no effect on actin-activated ATPase activity (*40*). It should be noted that, unlike smooth and scallop myosin, natural isoforms of *Dictyostelium* loop 1 do not exist in nature, perhaps explaining the disparate observations.

Conversely, ADP release and motility can vary despite two myosins having the same or similar loop 1 sequences. Rat β-cardiac myosin and pig β-cardiac myosin have only one conservative substitution (E to D) in loop 1, yet showed a 3−4-fold difference in ADP release rates and unloaded shortening velocity (*41*). This result suggests that sequence differences in other parts of the cardiac heavy chain must be responsible for the same changes evoked by loop 1 isoforms in smooth and scallop myosins. More importantly, these results imply that the structural features that determine ADP release rates, rates of in vitro motility, and actin-activated ATPase activity may differ even among myosins of class II.

The increase in positive charge in loop 2 of smHMM decreased the rate of in vitro motility and ADP release, despite this mutant having the same loop 1 as WT smHMM (Figure 4). This result implies that even in myosins where loop 1 affects ADP release and motility, loop 1 is not the sole determinant of these parameters as previously postulated (*17*). Most of the slowing of motility could be accounted for by a decreased rate of ADP release from actoHMM, which is the step that is considered to be rate-limiting for in vitro motility. In support of this contention, the rate of ADP release showed a linear correlation with the rate of motility. To a more minor extent, the increased charge of loop 2 could contribute to slowing of motility by virtue of these weak binding bridges exerting more of a "drag" on the cycling bridges. In nature, it is likely that the charge of loop 2 has been optimized to provide sufficent affinity for actin under physiological conditions, without imposing an unnecessary load on cycling bridges.

Interplay between the Actin- and Nucleotide-Binding Regions. The decrease in the rate of ADP release by the mutant with increased positive charge in loop 2 implies that there is communication between the actin-binding interface and the nucleotide-binding pocket. The idea of communication between these two regions was first hypothesized over 20 years ago on the basis of results from fluorescence resonance energy transfer and cross-linking experiments (*42*) and is supported by more recent structural studies. The cleft between the upper and lower 50 kDa regions of the motor domain is thought to provide the major route of communication between the actomyosin interface and the nucleotide-binding pocket (*1*, *2*, *43*). Evidence from electron cryo-

microscopy suggests that the cleft is partially closed in the actin-bound MgADP state and becomes more tightly closed after ADP release by movement of the upper 50 kDa region (*15*). MgATP binding then presumably dissociates actomyosin by opening the cleft; this is the most classic example of communication between these two regions.

Loop 1 can also influence how actin binding affects the affinity of myosin for MgADP. Scallop striated and catch myosins, which differ in loop 1, have the same affinity for ADP in the absence of actin (*39*). In the presence of actin, however, the affinity for ADP was 9-fold weaker for striated than for catch muscle S1. Similarly, smHMMs that differ by a seven amino acid insert in loop 1 had very similar affinities for ADP in the absence of actin, but in the presence of actin, the inserted form had a 13-fold weaker affinity for ADP compared to the noninserted form (*44*). In both cases, loop 1 seems to be altering the communication between the actin-binding interface and the nucleotide pocket and modulating the effect that strong actin binding has on ADP affinity. Structural studies also show that loop 1 becomes stabilized upon interaction with actin, despite its distance from the actomyosin interface (*15*).

What Features Determine V_{max}? V_{max} is determined by the rate-limiting P_i release step, as myosin goes from a weak to a strong binding state. If loop 2 does not determine V_{max}, what regions of the molecule do? As discussed above, V_{max} varies between loop 1 isoforms in smooth myosin and in scallop myosin. In addition, several regions of myosin are implicated in the strong binding interface with actin, and mutations in these regions have been shown to have a large impact on V_{max}. One of these regions is the HCM (hypertrophic cardiomyopathy) loop in the upper 50 kDa region, and the other is a cluster of hydrophobic residues in the lower 50 kDa region of myosin, in a helix−turn−helix motif (*15*). At the tip of the HCM loop there is a conserved negatively charged amino acid (or phosphorylatable residue). Mutation of this residue (D399A) in human nonmuscle myosin IIA HMM reduced V_{max} 10-fold (*45*). The same mutation (D403A) in *Dictyotelium* myosin II reduced V_{max} 3.3-fold (*46)*. Thus this negatively charged residue appears to have a role in the transition that allows P_i release. The R403Q mutation that results in familial hypertrophic cardiomyopathy (FHC) also causes an approximately 2-fold increase in V_{max} when engineered into the smHMM backbone (*47*). Mutation of any of the three hydrophobic residues WFP (residues 546−548 of smHMM) in the lower 50 kDa region to alanine essentially abolishes actin-activated ATPase activity (*48*). Conversely, mutation of the nearby TNPP (residues 532−535) to methionine enhances V_{max} by 2-fold (*48*), suggesting that the proline bulge contributes to lowering the enzymatic activity of smHMM. This list of mutations is not exhaustive but serves to highlight the point that other regions of the molecule contribute to determining V_{max}.

We conclude that the primary role of loop 2 is to determine the affinity of actin for myosin, without necessarily altering V_{max}. Conversely, loop 1 affects ADP release and in vitro motility but is not the sole regulator of these parameters. In our view, control of the kinetic and mechanical properties of myosin is influenced by multiple regions of the molecule, and the "rules" determined for one myosin and its closely related isoforms may not hold true for more distantly related myosins in the same class.

REFERENCES

1. Geeves, M. A., and Holmes, K. C. (1999) *Annu. Rev. Biochem. 68*, 687−728.
2. Houdusse, A., and Sweeney, H. L. (2001) *Curr. Opin. Struct. Biol. 11*, 182−194.
3. Siemankowski, R. F., Wiseman, M. O., and White, H. D. (1985) *Proc. Natl. Acad. Sci. U.S.A. 82*, 658−662.
4. Weiss, S., Rossi, R., Pellegrino, M.-A., Bottinelli, R., and Geeves, M. A. (2001) *J. Biol. Chem. 276*, 45902−45908.
5. Chaussepied, P. (1989) *Biochemistry 28*, 9123−9128.
6. Yamamoto, K. (1990) *Biochemistry 29*, 844−848.
7. Cheung, P., and Reisler, E. (1992) *Biochem. Biophys. Res. Commun. 189*, 1143−1149.
8. Schröder, R. R., Manstein, D. J., Jahn, W., Holden, H., Rayment, I., Holmes, K. C., and Spudich J. A. (1993) *Nature 364*, 171−174.
9. Sutoh, K., Ando, M., Sutoh, K., and Toyoshima, Y. Y. (1991) *Proc. Natl. Acad. Sci. U.S.A. 88*, 7711−7714.
10. Furch, M., Geeves, M. A., and Manstein, D. J. (1998) *Biochemistry 37*, 6317−6326.
11. Knetsch, M. L. W., Uyeda, T. Q. P., and Manstein, D. J. (1999) *J. Biol. Chem. 274*, 20133−20138.
12. Miller, C. J., and Reisler, E. (1995) *Biochemistry 34*, 2694−2700.
13. Miller, C. J., Wong, W. W., Bobkova, E., Rubenstein, P. A., and Reisler, E. (1996) *Biochemistry 35*, 16557−16565.
14. Wong, W. W., Doyle, T. C., and Reisler, E. (1999) *Biochemistry 38*, 1365−1370.
15. Volkmann, N., Hanein, D., Ouyang, G., Trybus, K. M., DeRosier, D. J., and Lowey, S. (2000) *Nat. Struct. Biol. 7*, 1147−1155.
16. Joel, P. B., Trybus, K. M., and Sweeney, H. L. (2001) *J. Biol. Chem. 276*, 2998−3003.
17. Spudich, J. A. (1994) *Nature 372*, 515−518.
18. Murphy, C. T., and Spudich, J. A. (2000) *J. Muscle Res. Cell Motil. 21*, 139−151.
19. Uyeda, T. Q. P., Ruppel, K. M., and Spudich, J. A. (1994) *Nature 368*, 567−569.
20. Murphy, C. T., and Spudich, J. A. (1999) *Biochemistry 38*, 3785−3792.
21. Takahashi, M., Takahashi, K., Hiratsuka, Y., Uchida, K., Yamagishi, A., Uyeda, T. Q. P., and Yazawa, M. (2001) *J. Biol. Chem. 276*, 1034−1040.
22. Rovner, A. S., Freyzon, Y., and Trybus, K. M. (1995) *J. Biol. Chem. 270*, 30260−30263.
23. Rovner, A. S. (1998) *J. Biol. Chem. 273*, 27939−27944.
24. Kolodziej, P. A., and Young, R. A. (1991) *Methods Enzymol. 194*, 508−519.
25. O'Reilly, D. R., Miller, L. K., and Luckow, V. A. (1992) *Baculovirus Expression Vectors, A Laboratory Manual*, W. H. Freeman, New York.
26. Laemmli, U. K. (1970) *Nature 227*, 680−685.
27. Perrie, W. T., and Perry, S. V. (1970) *Biochem. J. 119*, 31−38.
28. Trybus, K. M. (2000) *Methods 22*, 327−335.
29. Trybus, K. M., and Henry, L. (1989) *J. Cell Biol. 109*, 2879−2886.
30. White, H. D. (1982) *Methods Enzymol. 85*(Part B), 698−708.
31. Yengo, C. M., and Sweeney, H. L. (2002) *Biophys. J. 82*, 408a−409a.
32. Asukagawa, H., and Sutoh, K. (2002) *Results Probl. Cell Differ. 36*, 65−74.
33. Goodson, H. V., Warrick, H. M., and Spudich, J. A. (1999) *J. Mol. Biol. 287*, 173−185.
34. Kelley, C. A., Takahashi, M., Yu, J. H., and Adelstein, R. S. (1993) *J. Biol. Chem. 268*, 12848−12854.
35. Rovner, A. S., Freyzon, Y., and Trybus, K. M. (1997) *J. Muscle Res. Cell Motil. 18*, 103−110.
36. Sweeney, H. L., Rosenfeld, S. S., Brown, F., Faust, L., Smith, J., Xing, J., Stein, L. A., and Sellers, J. R. (1998) *J. Biol. Chem. 273*, 6262−6270.
37. Rovner, A. S., Fagnant, P. M., and Trybus, K. M. (2003) *J. Biol. Chem.* (in press).
38. Perreault-Micale, C. L., Kalabokis, V. N., Nyitray, L., and Szent-Györgyi, A. G. (1996) *J. Muscle Res. Cell Motil. 17*, 543−553.
39. Kurzawa-Goertz, S. E., Perreault-Micale, C. L., Trybus, K. M., Szent-Györgyi, A. G., and Geeves, M. A. (1998) *Biochemistry 37*, 7517−7525.
40. Murphy, C. T., and Spudich, J. A. (1998) *Biochemistry 37*, 6738−6744.

41. Sant'Ana Pereira, J., Pavlov, D., Patel, J. R., Greaser, M., Homsher, E., and Moss, R. (2000) *Biophys. J. 78*, 273A.
42. Morales, M. F., and Botts, J. (1979) *Proc. Natl. Acad. Sci. U.S.A. 76*, 3857−3859.
43. Fisher, A. J., Smith, C. A., Thoden, J., Smith, R., Sutoh, K., Holden, H. M., and Rayment, I. (1995) *Biophys. J. 68*, 19s−28s.
44. Geeves, M. A., Berger, C., Fagnant, P., and Trybus, K. (2002) *Biophys. J. 82*, 374a.
45. Wang, F., Harvey, E. V., Conti, M. A., Wei, D., and Sellers, J. R. (2000) *Biochemistry 39*, 5555−5560.
46. Sasaki, N., Asukagawa, H., Yasuda, R., Hiratsuka, T., and Sutoh, K. (1999) *J. Biol. Chem. 274*, 37840−37844.
47. Yamashita, H., Tyska, M. J., Warshaw, D. M., Lowey, S., and Trybus, K. M. (2000) *J. Biol. Chem. 275*, 28045−28052.
48. Kojima, S., Konishi, K., Katoh, K., Fujiwara, K., Martinez, H. M., Morales, M. F., and Onishi, H. (2001) *Biochemistry 40*, 657−664.

BI034415J